

Comparative Visualization for Comprehensive Two-Dimensional Gas Chromatography^{*}

Benjamin V. Hollingsworth^a, Stephen E. Reichenbach^{b,*}

^a*GC Image LLC, PO Box 57403, Lincoln NE 68505-7403, USA*

^b*Computer Science and Engineering Department, University of Nebraska – Lincoln, Lincoln NE 68588-0115, USA*

Abstract

This paper investigates methods for comparing two datasets produced by comprehensive two-dimensional gas chromatography (GCxGC). Chemical comparisons are useful for process monitoring, sample classification or identification, correlative determinations, and other important tasks. GCxGC is a powerful new technology for chemical analysis, but methods for comparative visualization must address challenges posed by GCxGC data: inconsistency and complexity. The approach extends conventional techniques for image comparison by utilizing specific characteristics of GCxGC data and developing new methods for comparative visualization and analysis. The paper describes techniques that register (or align) GCxGC datasets to remove retention-time variations; normalize intensities to remove sample amount variations; compute differences in local regions to remove slight misregistrations and differences in peak shapes; employ color (hue), intensity, and saturation to simultaneously visualize differences and values; and use tools for masking, three-dimensional visualization, and tabular presentation with controls for graphical highlights to significantly improve comparative analysis of GCxGC datasets.

Key words: Gas chromatography, comprehensive two-dimensional; GCxGC; Comparative visualization; Comparative analysis

^{*} This work was supported by the NIH National Center for Research Resources (1 R43 RR020256-01) and by the NSF Science and Engineering Information Integration and Informatics Program (IIS-0431119).

^{*} Tel.: +1.402.472.5007; fax: +1.402.472.7767

Email address: reich@cse.unl.edu (Stephen E. Reichenbach).

1 Introduction

This paper investigates methods for comparing two datasets produced by comprehensive two-dimensional gas chromatography (GCxGC). Chemical comparisons are useful for process monitoring, sample classification or identification, correlative determinations, and other important tasks. GCxGC [1] is a powerful new chemical separation technology that provides significant advantages over traditional GC: an order-of-magnitude increase in chemical separation capacity, higher-dimensional chemical ordering, and a significant increase in signal-to-noise ratio. GCxGC has important potential uses for comparative chemical analysis, for example:

- comparing manufactured products with standards for quality control [2];
- monitoring actual or potential pollution sites for environmental changes [3];
- surveying crime scenes for chemical “fingerprints” [4]; and
- assaying classes of tissue samples for biomarker discovery [5].

However, the lack of software for GCxGC data and information processing has been a significant impediment to the adoption of GCxGC for routine applications [6].

This paper addresses two challenges for computer-based comparative visualization and analysis of GCxGC datasets: data inconsistency and complexity. First, GCxGC datasets exhibit inconsistencies in sample amounts, peak retention times, and peak shapes that are caused by uncontrolled chromatographic variations and which are not related chemical differences in the samples. If these incidental variations are not removed from the comparison, they can confound and obscure actual chemical differences. Second, even if incidental inconsistencies are removed, the chemical comparisons typically are complex and difficult to visualize and report. In particular, GCxGC data may contain thousands of peaks in complex multi-dimensional patterns related to chemical structure. Moreover, different comparative aspects, such as absolute differences or relative differences, may be more or less important for different chemicals and for different applications. Presenting complex comparisons of complex data on a computer monitor (or printed page) is challenging.

The approach in this paper is to extend conventional techniques for image comparison by utilizing specific characteristics of GCxGC data and developing new methods for comparative visualization and analysis. GCxGC data can be represented, visualized, and processed as an image, *e.g.*, $a[m, n]$ where a is the analyzed image with pixels indexed by first-column retention-time m (increasing left-to-right) and second-column retention-time n (increasing bottom-to-top). As in Fig. 1, each resolved compound produces a small two-dimensional peak with pixel values (or intensities) that are larger than the

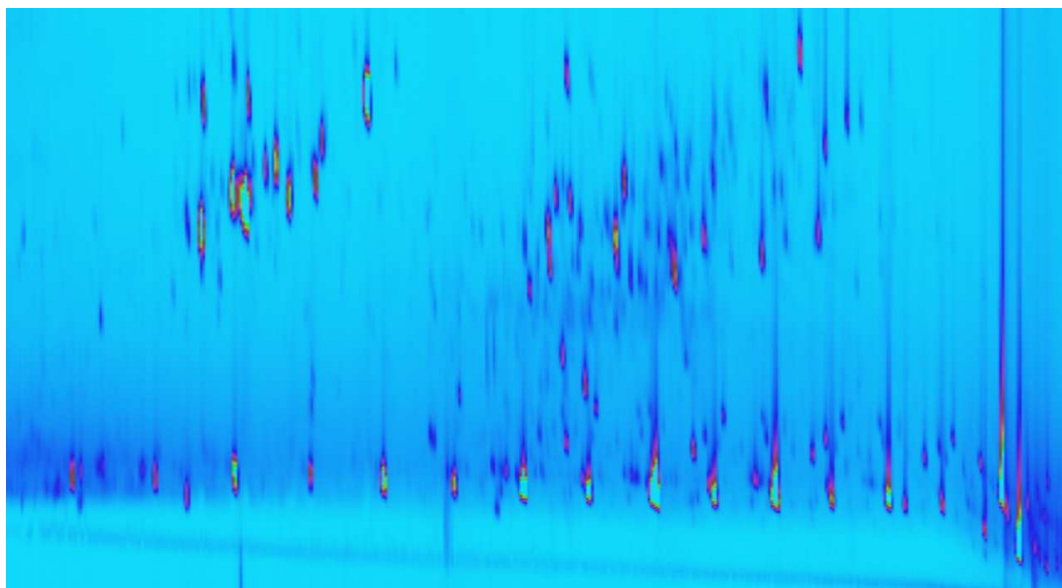


Fig. 1. Reference image for comparison.

background values and can be visually distinguished through pseudo-color mapping of the pixel values. Then, two GCxGC datasets can be compared by simple techniques, such as side-by-side comparison or flicker (*i.e.*, alternating) between images [7], or by digital image processing methods, such as creating a difference image (by subtraction) or addition image (by addition in different colors) [8,9,10]. The pixel values also can be interpreted as elevation, generating a three dimensional surface which can be projected to two dimensions for visualization.

The methods developed in Section 2 use GCxGC metadata, such as peak identifications and quantifications, to *register* (*i.e.*, align) retention times between two data sets (correcting for incidental variations of retention times) and to *normalize* values between two data sets (correcting for incidental differences in sample amounts). Section 3 develops a new *colorized difference* method to visually emphasize the remaining differences and a new *fuzzy difference* method that can be used to suppress variations of peak shape in order to highlight differences in chemical composition. Section 4 describes an interactive peak comparison table that provides analysts with quantitative data and control of peak-oriented graphical overlays and an interactive environment for three-dimensional viewing that enables analysts to combine comparison methods using elevation. Section 5 examines issues for further research and development.

2 Data Processing

This paper considers comparisons between two GCxGC images — the dataset currently selected for analysis, referred to as the *analyzed image*, is compared to another image, referred to as the *reference image*. Prior to comparison, each image is processed separately to correct acquisition artifacts (*e.g.*, background removal [11]) and to detect, identify, and quantify chemical peaks [6]. Then, two additional data processing steps are performed on the reference image to remove incidental differences with the analyzed image. Section 2.1 describes transformation of retention times to register identified peaks in the reference image to corresponding peaks in the analyzed image. Section 2.2 describes value (or intensity) scaling to normalize the response (*i.e.*, total peak intensity) for quantitative standard(s) in the reference image to the response for standard(s) in the analyzed image. These two steps are critical for suppressing incidental variations and emphasizing only real chemical differences.

2.1 Registration

Registration consists of two steps: (1) determine a transformation of the reference image to remove differences in retention times and (2) resample the transformed reference image at the pixel locations of the analyzed image.

Various two-dimensional geometric transformations have been used for digital image processing [12]. Affine transformation has been shown to effectively remove retention variations related to chromatographic parameters [13]. The transformed two-dimensional retention times (x_t, y_t) are computed from the reference image retention times (x_r, y_r) as:

$$\begin{bmatrix} x_t \\ y_t \end{bmatrix} = \begin{bmatrix} a & b \\ c & d \end{bmatrix} \begin{bmatrix} x_r \\ y_r \end{bmatrix} + \begin{bmatrix} e \\ f \end{bmatrix}, \quad (1)$$

where (a, b, c, d, e, f) are the parameters of affine transformation.

The parameters of affine transformation can be fit to minimize the mean-square difference between the transformed retention times of a set of identified peaks in the reference image and the retention times of the corresponding peaks (*i.e.*, the peaks with the same chemical identities) in the analyzed image. Let B be a set of corresponding peaks b_i , such that each peak is present and uniquely identified in both the analyzed and reference images with retention times $(x_a(b_i), y_a(b_i))$ and $(x_r(b_i), y_r(b_i))$, respectively. Then, the parameters of the transformation are set to minimize:

$$E = \frac{1}{|B|} \sum_{b_i \in B} \sqrt{(x_a(b_i) - x_t(b_i))^2 + (y_a(b_i) - y_t(b_i))^2}. \quad (2)$$

Registration could be made more precise by using locally adaptive transformations rather than a global transformation, but locally adaptive registration is more sensitive to errors.

One possible problem is that mismatched pairs of peaks (*e.g.*, due to misidentification) can reduce the accuracy of the transformation. To avoid this, after the first transformation is computed from the set of all corresponding peaks, the peaks for which the transformed retention times differ most from the corresponding-peak retention times in the analyzed image are removed from the peak set and the least-squares fit is recomputed on the remaining peaks. Observations suggest that removing the 25% of peak pairs with the largest differences effectively removes mismatched pairs. At least three non-colinear points must be retained in the peak set to uniquely determine the optimal affine transformation.

The reference image is then transformed, interpolated, and resampled at the pixel locations of the analyzed image. Interpolating by convolution yields the transformed image t :

$$t[x_t, y_t] = \sum_{m', n'} r[m', n'] f(x_r - m', y_r - n'), \quad (3)$$

where r is the reference image and f is the interpolation function. Bilinear interpolation is a simple, yet effective two-dimensional interpolator [14].

2.2 Normalization

For two runs (even from the same sample), slightly different sample amounts are introduced and so produce different responses. Differences in GCxGC images due to variable sample amounts must be corrected so that they are not mistaken as differences in concentrations.

GCxGC intensities are relatively linear with respect to amount, so normalization can be implemented by multiplicative scaling. The scale factor is set to equalize the response in the analyzed and reference images to one or more quantitative standards which are taken to have the same concentrations in both samples. For example, in analyzing chemical changes over time at the site an oil spill, Reddy *et al.* [3] used hopane as a quantitative standard for comparisons because it is relatively persistent over the observation period.

Given a set S of peaks b_i for quantitative standards that are identified and

quantified in both the analyzed and reference images, where $V_a(b_i)$ is the detected volume (total peak response) in the analyzed image and $V_r(b_i)$ is the detected volume in the reference image, the scale factor is computed as:

$$F = \frac{\sum_{b_i \in S} V_a(b_i)}{\sum_{b_i \in S} V_r(b_i)}. \quad (4)$$

Just as for registration, mismatched pairs of peaks can reduce the accuracy of normalization. The same method for avoiding registration errors can be used to avoid normalization errors. The scale factor is first computed for all quantitative standards. Then, the scale factor is applied to the individual volumes of the quantitative peaks in the reference image. The 25% of quantitative standards with the greatest difference magnitude between the scaled reference volume and the analyzed volume are removed from the set of quantitative standards and the scale factor is recomputed.

The scale factor is applied to each pixel of the transformed reference image:

$$s[m, n] = F \cdot t[m, n] \quad (5)$$

The transformed and scaled reference image s now can be compared to the analyzed image a .

3 Image-Based Comparison Methods

This section illustrates several image-based comparison methods using two images from samples collected by Reddy *et al.* [3] at varying depths of the intertidal marsh sediment affected by an oil spill. (The data presented here to illustrate visualization is from preliminary runs. Subsequent runs, with improved GCxGC settings, are in [3].) The data for the analyzed image was acquired at a depth of 0–4cm and the data for the reference image was acquired at a depth of 16–20cm. The subimage of the reference image used for visualization is shown in Fig. 1. The n -alkanes from C₂₂ form a regular pattern along the bottom of the image and more polar natural (*i.e.*, not introduced by the oil spill) compounds appear in the top half of the image. The reference image was registered to the analyzed image using a peak set containing several n -alkanes, the solvent peak, and a well-separated peak among the natural polar compounds. The reference image was normalized to the analyzed image using a peak set of n -alkanes. This creates a set of peaks with nearly

equal responses and (as will be seen) yields one set of natural compound peaks which are more prominent in the reference image and another set of natural compound peaks which are more prominent in the analyzed image.

3.1 Grayscale Difference

A popular method for comparing two images is to form a *difference image* by subtracting the individual pixel values of one image from the corresponding pixel values of the other image [8]. The comparison techniques developed in this paper extend the difference image method.

In these comparisons, the reference image is subtracted from the analyzed image, so a positive difference indicates that the analyzed image has a larger pixel value and a negative difference indicates that the reference image has a larger pixel value. The difference image can be displayed with a grayscale so that medium gray represents zero difference, brighter values represent positive differences, and darker values represent negative differences. The larger the magnitude of the difference, the closer the displayed pixel is to white or black. A logarithmic scale can be used to better highlight differences with smaller magnitudes, but the same scale factor is used for both positive and negative values. An example grayscale difference image is shown in Fig. 2. The cluster of peaks in the upper-left are mostly dark, indicating the reference image has greater intensity; the cluster of peaks in the upper-right are mostly bright, indicating that the analyzed image has greater intensity; and the *n*-alkane peaks along the bottom have both bright and dark, so the relative intensities are not clear.

The grayscale difference method does an adequate job of showing the differ-

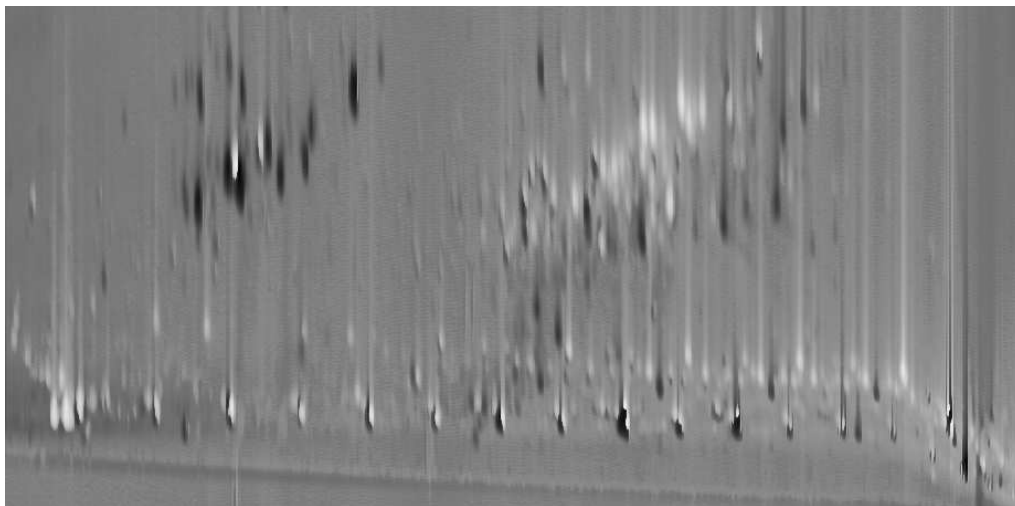


Fig. 2. Grayscale difference image.

ences between the two images, but the relative context of those differences is lost because the magnitude of the original pixel values is not represented in the output image (only the difference). Another problem is indicated by the adjacent bright and dark areas (especially for the n -alkane peaks). These adjacent areas with opposite colors are due to slight misregistration or slight peak shape differences.

3.2 Colorized Difference

In order to make the differences between the analyzed and reference images more apparent and to retain some context for those differences, the traditional grayscale difference method is modified to color code the differences and incorporate the original image pixel intensities. First, the difference image is computed, just as it is for the grayscale difference method. Then, for display, the difference image is converted into a 24-bit color image (three separate bands of 8-bit integers). The color is computed in Hue-Intensity-Saturation (HIS) space [15]. The hue component of each pixel is set to pure green if the analyzed pixel value is larger or pure red if the reference pixel value is larger. The intensity component of each pixel is the maximum of the original analyzed and reference pixel values, scaled to fit into the 0–1.0 range. The saturation component of each pixel is the magnitude of the difference value, scaled to fit into the 0–1.0 range. After the hue, intensity, and saturation components are calculated for each pixel, they are converted to the RGB color space and stored in a 24-bit image.

An example colorized difference image is shown in Fig. 3. The resulting color image shows brighter pixels (larger intensity) where either of the original images have larger values and darker pixels (smaller intensity) where both of

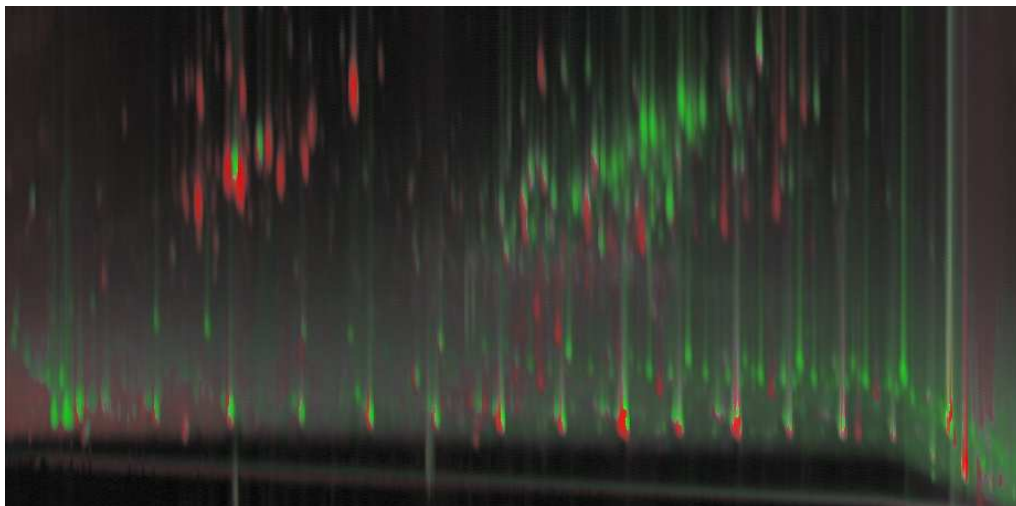


Fig. 3. Colorized difference image.

the original images have smaller values, thereby retaining context for the differences that is lacking in the grayscale difference method. Pixels that have approximately equal values in both original images appear grayish (smaller saturation), whereas pixels for which there is a large difference have bolder colors (larger saturation). This allows the user to see simultaneously peak heights and peak differences. The problem of peaks with adjacent positive and negative values still is evident.

3.3 Fuzzy Difference

In practice, differences between analyzed and reference images may be caused by slight misregistration or slightly different peak shapes. It is desirable to suppress these differences so that differences in chemical concentrations are seen more clearly. These differences can be reduced by a new *fuzzy difference* comparison. Rather than comparing pixels one-by-one, the fuzzy difference method compares each pixel value in one image with the values in a small neighborhood of the other image.

To compute the fuzzy difference between the two images, the user specifies the size of a small, rectangular window which defines a neighborhood around each pixel. The difference value at each pixel in the output image is computed using a three-step process. The first two steps compute two intermediate difference images — one comparing pixels in the analyzed image with neighborhoods in the reference image and one comparing pixels in the reference image with neighborhoods in the analyzed image. First, for each pixel, the difference is computed between that pixel value in the analyzed image and the minimum and maximum values found in the neighborhood window of the reference image. That is, for each pixel location $[m, n]$, analyzed pixel value $a[m, n]$, transformed and scaled reference pixel value $s[m, n]$, and window $w_s\{[m, n]\}$, the difference pixel value $d_a[m, n]$ is:

$$\begin{aligned}
 s_{max}[m, n] &= \max_{[m', n'] \in w_s\{[m, n]\}} (s[m', n']) \\
 s_{min}[m, n] &= \min_{[m', n'] \in w_s\{[m, n]\}} (s[m', n']) \\
 \text{if } a[m, n] < s_{min}[m, n], &\text{ then } d_a[m, n] = a[m, n] - s_{min}[m, n] \\
 \text{else if } a[m, n] > s_{max}[m, n], &\text{ then } d_a[m, n] = a[m, n] - s_{max}[m, n] \\
 \text{else } d_a[m, n] &= 0
 \end{aligned}$$

A difference is recorded only if the analyzed pixel value is either larger or smaller than *all* of the reference pixel values in the surrounding window. This allows the fuzzy difference algorithm to compensate for misaligned or differently shaped peaks while still showing differences in peak heights. The neighborhood window size should be set no larger than one peak width in each dimension so that pixel neighborhoods do not overlap multiple peaks. Second,

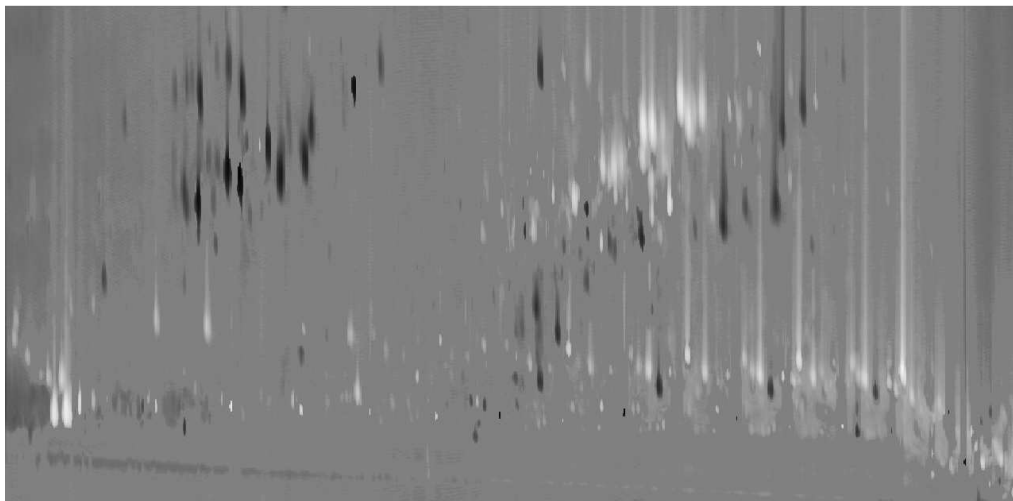


Fig. 4. Grayscale fuzzy difference image.

the same intermediate difference algorithm is then repeated, with the analyzed and reference images swapping roles.

In the third step, the pixel values in the final fuzzy difference image are determined by whichever intermediate difference image has the largest magnitude. If the image that used the reference pixel as the center of each window is selected, its pixel value is negated in order to retain the same positive/negative relationship as the traditional difference image.

The fuzzy difference image can be converted to an 8-bit integer image for display, using the same method employed for the traditional grayscale difference comparison method detailed in Section 3.1. An example fuzzy difference image is shown in Fig. 4. In this image, it is clear that most of the n -alkane peaks (along the bottom of the image) have nearly equal intensity in both images. However, the grayscale shows only the difference, so it is not apparent that the n -alkane peaks are large in value as well as similar in intensity.

The fuzzy difference image also can be displayed with the colorized difference method described in Section 3.2. An example of the colorized fuzzy difference image is shown in Fig. 5. The colorized fuzzy difference image removes many spurious differences by compensating for misaligned or differently shaped peaks and provides additional context for the difference values. The colorized fuzzy difference algorithm effectively highlights the most interesting differences, even where peaks are slightly misaligned or differently shaped. It is also clear that the n -alkane peaks are large in magnitude.

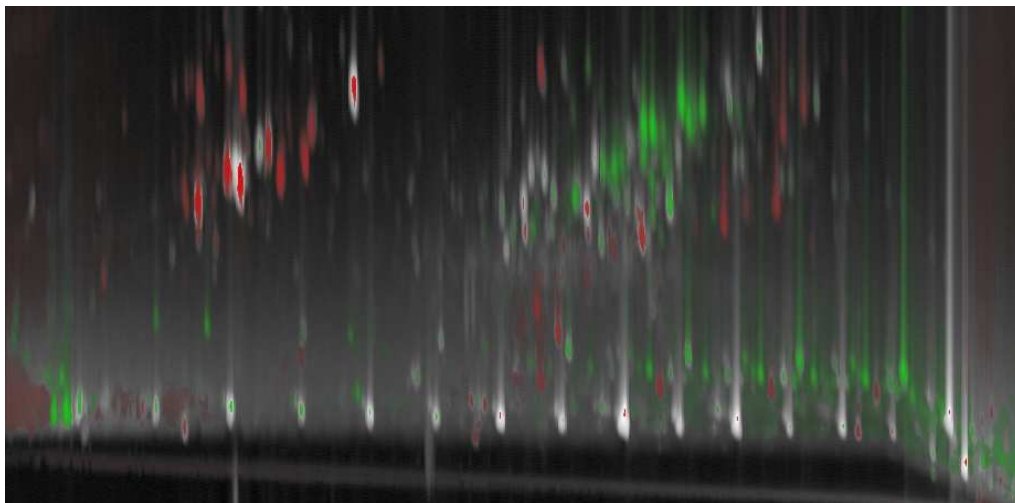


Fig. 5. Colorized fuzzy difference image.

4 Tools for Comparative Analysis

Once comparison images have been generated for any of the image-based methods, additional tools can enhance the user's understanding of the data.

4.1 Masking

The comparison process attempts to highlight interesting differences and suppress other differences. Users may want to mask (block) certain areas of an image so that comparisons are displayed only for a particular region(s) of the image. This is especially important if the scale of uninteresting differences is much larger than differences of interest. Masking tools allow users to delineate geometric regions or designate peak subsets to be excluded from comparison. Pixels in masked areas are set to a null value appropriate for the currently selected comparison method (*e.g.*, gray for grayscale difference and black for colorized difference).

4.2 Tabular Data

Tabular comparisons can provide quantitative information that cannot be communicated in image-based comparisons. A comparative table provides important statistical data for each pair of peaks that are uniquely identified in both the analyzed and reference image, such as volume (*i.e.*, total response), area (*i.e.*, number of pixels), peak retention times, and value at the peak pixel. For each feature, the values for the analyzed and reference image are listed

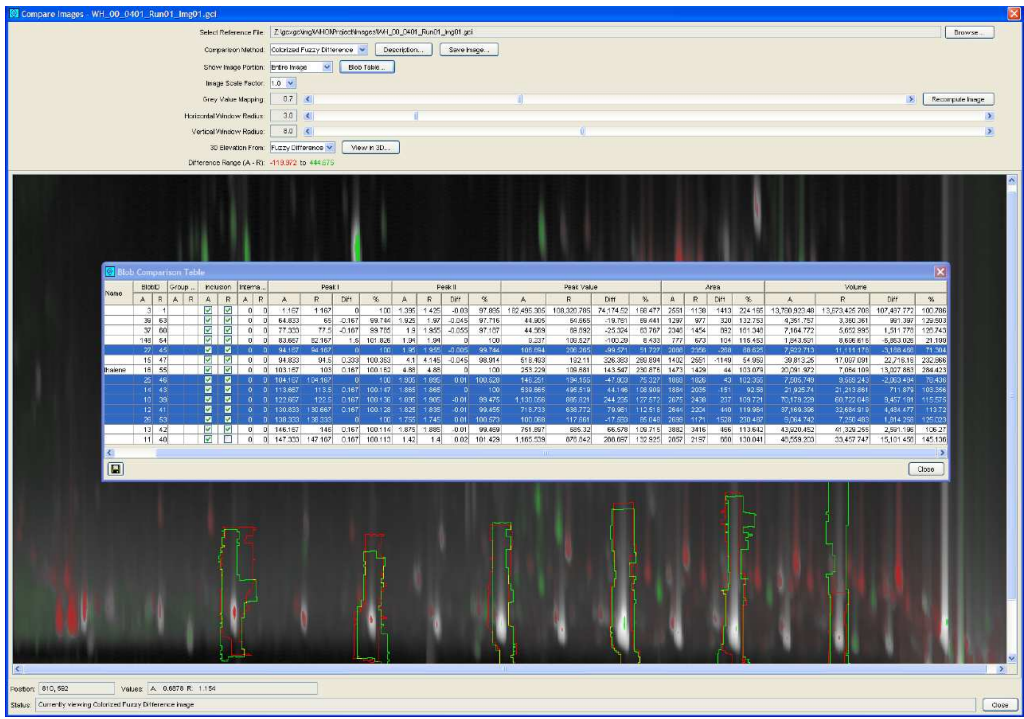


Fig. 6. Tabular and image views with selected peaks.

side-by-side in the table, along with the differences (both absolute and percentage). To aid in analysis, the table rows may be sorted on any feature for either image or on any difference. The contents of the table may be saved to a file formatted as ASCII comma-separated values (CSV) for later importation into spreadsheet, database, or word-processing applications.

Visual comparisons and tabular comparisons each have advantages, so it is useful to navigate between the two views. If one or more peaks in the table are selected (with the mouse), those rows are graphically highlighted in the image by outlines drawn on the comparison image. This allows the user to easily locate peaks of interest, for example, the peaks with the largest volume difference or the peaks with the largest percent difference. Fig. 6 illustrates a tabular view with selected peaks and corresponding image with graphical highlights.

4.3 Three-Dimensional Visualization

GCxGC image data can be visualized as an elevation map, with peaks appearing as mountains. In this view, value is shown as elevation, which allows colorization to be used for other aspects of the data. For the elevation map, the user may select one of four different images: the original analyzed image, the transformed and scaled reference image, the difference image, or

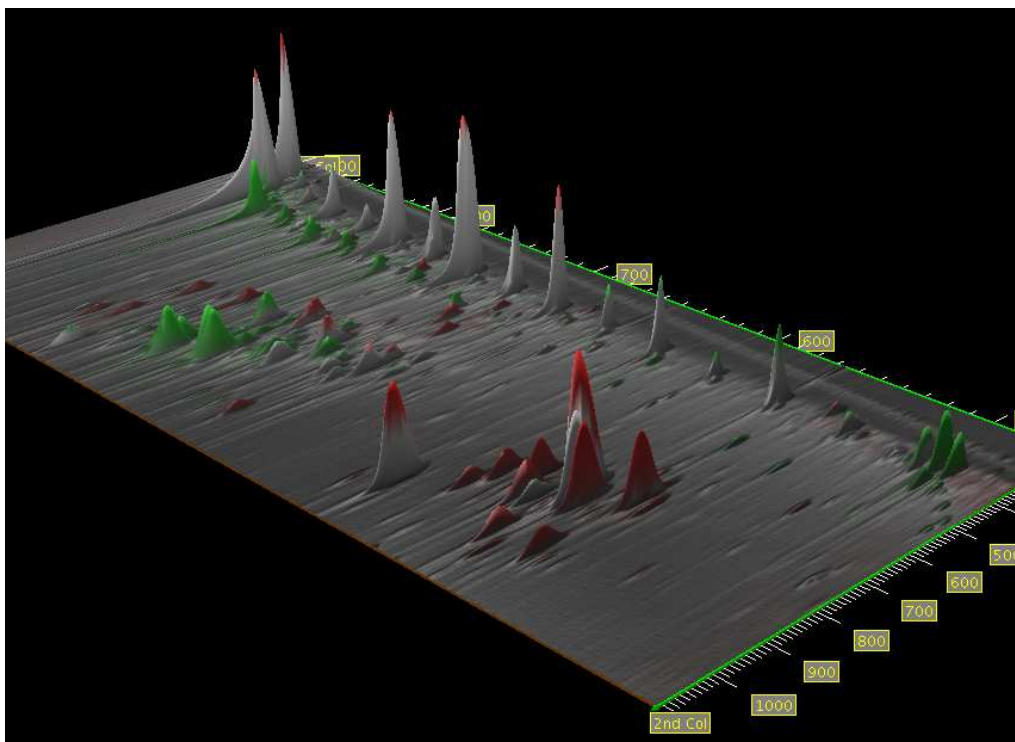


Fig. 7. Three-dimensional rendering of a colorized fuzzy difference image draped over a maximum value elevation map.

an image with each pixel set to the larger of either the analyzed or reference image pixel. Masked areas or peaks are set to zero elevation. The color overlay that is draped over the surface of the elevation map can be set by the grayscale difference, colorized difference, or other difference (*e.g.*, percentage difference). The ability to drape any comparison image over different elevation maps provides great versatility in analyzing the data. It also allows even the grayscale difference comparisons (traditional or fuzzy) to be viewed in the context of the original pixel data — something that is not possible using only a two-dimensional image. The user can then view the data from various distances or viewing angles and can locate the viewer’s position anywhere in or around the data. A sample three-dimensional view is shown in Fig. 7.

5 Conclusion

This paper develops new methods for comparing datasets produced by GCxGC. Methods for registration and scaling remove incidental variations in retention times and sample amounts based on GCxGC peak metadata. A colorized difference method simultaneously shows pixel differences and pixel values. A fuzzy difference method removes incidental variations in peak shapes and peak alignments based on values in a local neighborhood. Tools for masking, tab-

ular metadata, and three-dimensional visualization significantly improve interactive analyses. Ongoing work is developing new methods for model-based GCxGC analyses and comparisons.

References

- [1] W. Bertsch, Two-dimensional gas chromatography. Concepts, instrumentation, and applications — Part 2: Comprehensive two-dimensional gas chromatography, *Journal of High Resolution Chromatography* 23 (3) (2000) 167–181.
- [2] R. Shellie, P. Marriott, A. Chaintreau, Quantitation of suspected allergens in fragrances (Part I): evaluation of comprehensive two-dimensional gas chromatography for quality control triple-dimensional analysis of complex volatile samples, *Flavour and Fragrance Journal* 19 (2) (2004) 91–98.
- [3] C. M. Reddy, T. I. Eglinton, A. Hounshell, H. K. White, L. Xu, R. B. Gaines, G. S. Frysinger, The West Falmouth oil spill after thirty years: The persistence of petroleum hydrocarbons in marsh sediments, *Environmental Science and Technology* 36 (22) (2002) 4754–4760.
- [4] G. Frysinger, R. Gaines, Forensic analysis of ignitable liquids in fire debris by comprehensive two-dimensional gas chromatography, *Journal of Forensic Science* 47 (3) (2002) 471–482.
- [5] W. Welthagen, R. Shellie, M. Ristow, J. Spranger, R. Zimmermann, O. Fiehn, Comprehensive two dimensional gas chromatography – time of flight mass spectrometry, gcxgc-tof for high resolution metabolomics: Biomarker discovery on spleen tissue extracts of obese nzo compared to lean c57bl/6 mice, *Metabolomics* 1 (1) (2005) 57–65.
- [6] S. E. Reichenbach, M. Ni, V. Kottapalli, A. Visvanathan, Information technologies for comprehensive two-dimensional gas chromatography, *Chemometrics and Intelligent Laboratory Systems* 71 (2) (2004) 107–120.
- [7] P. Lemkin, L. Lipkin, B. Shapiro, M. Wade, M. Schultz, E. Smith, C. Merrill, M. van Keuren, W. Oertel, Software aids for the analysis of 2d gel electrophoresis images, *Computers and Biomedical Research* 12 (6) (1979) 517–44.
- [8] R. C. Gonzalez, R. E. Woods, *Digital Image Processing*, Addison-Wesley Publishing Company, Inc., 1992.
- [9] A. Kunzel, Controlled color coding in digital subtraction radiography, *CARS'99 Computer Assisted Radiology and Surgery. Proceedings of the 13th International Congress and Exhibition* (1999) 922–926.

- [10] X.-Q. Shi, I. Eklund, G. Tronje, U. Welander, H. Stamatakis, P.-E. Engstrom, G. Norhagen Engstrom, Comparison of observer reliability in assessing alveolar bone changes from color-coded with subtraction radiographs, *Dentomaxillofacial Radiology* 28 (1999) 31–36.
- [11] S. E. Reichenbach, M. Ni, D. Zhang, E. B. Ledford, Jr., Image background removal in comprehensive two-dimensional gas chromatography, *Journal of Chromatography A* 985 (1) (2003) 47–56.
- [12] M. Nadler, E. P. Smith, *Pattern Recognition Engineering*, John Wiley & Sons Ltd, 1993.
- [13] M. Ni, S. E. Reichenbach, A. Visvanathan, J. R. TerMaat, E. B. Ledford, Jr., Peak pattern variations related to GCxGC acquisition, *Journal of Chromatography A*.
- [14] A. Rosenfeld, A. C. Kak, *Digital Picture Processing*, 2nd Edition, Vol. 2, Academic Press, Inc., 1982.
- [15] J. D. Foley, A. van Dam, S. K. Feiner, J. F. Hughes, *Computer Graphics: Principles and Practice*, 2nd Edition, Addison-Wesley Publishing Company, Inc., 1990.
- [16] J. Phillips, J. Beens, Comprehensive two-dimensional gas chromatography: a hyphenated method with strong coupling between the two dimensions, *Journal of Chromatography A* 856 (1–2) (1999) 331–347.
- [17] E. B. Ledford, Jr., C. A. Billesbach, GC³: Comprehensive three-dimensional gas chromatography, *Journal of High Resolution Chromatography* 23 (3) (2000) 205–207.
- [18] M. Ni, S. Reichenbach, A statistics-guided progressive RAST algorithm for peak template matching in GCxGC, *Proceedings of the 2003 IEEE Workshop on Statistical Signal Processing* (2003) 383–386.